



Published in final edited form as:

*Angew Chem Int Ed Engl.* 2016 May 10; 55(20): 6071–6074. doi:10.1002/anie.201600521.

## Efficient Synthesis of Molecular Precursors for Parahydrogen-Induced Polarization of Ethyl Acetate-1-<sup>13</sup>C and Beyond

Roman V. Shchepin, Danila A. Barskiy, Aaron M. Coffey, Isaac V. Manzanera Esteve, and Eduard Y. Chekmenev

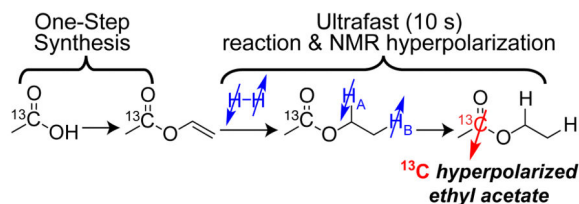
Department of Radiology, Vanderbilt University Institute of Imaging Science (VUIIS), Nashville, Tennessee, 37232, United States

Eduard Y. Chekmenev: [eduard.chekmenev@vanderbilt.edu](mailto:eduard.chekmenev@vanderbilt.edu)

### Abstract

Scalable and versatile methodology for production of vinylated carboxylic compounds with <sup>13</sup>C isotopic label in C1 position is described. It afforded robust synthesis of vinyl acetate-1-<sup>13</sup>C, which is a precursor for preparation of <sup>13</sup>C hyperpolarized ethyl acetate-1-<sup>13</sup>C, which provides a convenient vehicle for potential in vivo delivery of hyperpolarized acetate to probe metabolism in living organisms. Kinetics of vinyl acetate molecular hydrogenation and polarization transfer from parahydrogen to <sup>13</sup>C via magnetic field cycling were investigated. Nascent proton nuclear spin polarization (%*P<sub>H</sub>*) of ~3.3% and carbon-13 polarization (%*P<sub>13C</sub>*) of ~1.8% were achieved in ethyl acetate utilizing 50% parahydrogen corresponding to ~50% polarization transfer efficiency. The use of nearly 100% parahydrogen and the improvements of %*P<sub>H</sub>* of parahydrogen-nascent protons will likely enable production of <sup>13</sup>C hyperpolarized contrast agents with *P<sub>13C</sub>* of 20–50% in seconds using presented here chemistry for preparation of metabolically relevant precursors. Hyperpolarized in this fashion <sup>13</sup>C contrast agents can be employed for ultra-fast molecular imaging, the feasibility of which is presented here. A series of 3D images was acquired using <sup>13</sup>C hyperpolarized ethyl acetate-1-<sup>13</sup>C with high spatial (0.5 × 0.5 × 4 mm<sup>3</sup>) and temporal (~2.5 s) resolution.

### Graphical abstract



Scalable and versatile methodology for production of vinylated carboxylic compounds with <sup>13</sup>C isotopic label in C1 position is described. It afforded robust synthesis of vinyl acetate-1-<sup>13</sup>C, which is a precursor for preparation of <sup>13</sup>C NMR hyperpolarized ethyl acetate-1-<sup>13</sup>C. <sup>13</sup>C hyperpolarization of ~1.8% is achieved using Parahydrogen Induced Polarization Side Arm

Hydrogenation (PHIP-SAH). Production of metabolic  $^{13}\text{C}$  hyperpolarized contrast (with up to 50%  $^{13}\text{C}$  NMR polarization) in seconds is potentially feasible.

## Keywords

hyperpolarization;  $^{13}\text{C}$ ; PHIP; ethyl acetate; MRI

Hyperpolarized (HP) Molecular Resonance<sup>[1]</sup> is a rapidly growing field, which enables real-time metabolic imaging.<sup>[2]</sup> This is possible because nuclear spin polarization  $P$  of long-lived (on the order of a minute or more)  $^{13}\text{C}$  sites in biologically relevant molecules can be enhanced transiently by 4–8 orders<sup>[3]</sup> of magnitude to the order of unity or 100%. Dissolution Dynamic Nuclear Polarization (d-DNP)<sup>[3a]</sup> is one of the leading hyperpolarization technologies, which has advanced into clinical trials,<sup>[4]</sup> and its success has been largely driven by a wide range of biomolecules amenable for efficient hyperpolarization. Alternative hyperpolarization technique of Parahydrogen Induced Polarization (PHIP)<sup>[5]</sup> has two advantages over d-DNP: (i) fast production speed of < 1 minute vs. tens of minutes<sup>[6]</sup> to several hours, and (ii) it is significantly less instrumentation demanding.<sup>[7]</sup> Therefore, PHIP may potentially become an ultra-fast and low-cost hyperpolarization technique for affordable production of multiple doses of hyperpolarized (HP) contrast agents within minutes.<sup>[8]</sup> However, unlike d-DNP, PHIP technique relies on the pairwise addition of parahydrogen (*para*- $\text{H}_2$ ) to an unsaturated precursor usually followed by polarization transfer from nascent protons to  $^{13}\text{C}$  centers, with substantially longer  $P$  decay times ( $T_1$ ) required for *in vivo* applications.<sup>[9]</sup> While a number of metabolic  $^{13}\text{C}$  HP contrast agents have been developed for *in vivo* applications with % $P_{13\text{C}}$  10% in aqueous medium (e.g. succinate<sup>[2e, 10]</sup> and phospholactate<sup>[3b, 11]</sup>), PHIP remained relatively restricted technology because of the chemical challenge of inserting *para*- $\text{H}_2$  adjacently to  $^{13}\text{C}$  in molecular frameworks to yield metabolically relevant contrast agents: e.g. acetate, pyruvate, etc.<sup>[11a]</sup>

Recently PHIP using Side Arm Hydrogenation (SAH) was demonstrated,<sup>[12]</sup> where *para*- $\text{H}_2$  is added into vinyl moiety, and *para*- $\text{H}_2$ -derived polarization is transferred to carboxylic  $^{13}\text{C}$ . This is fundamentally possible, because in PHIP-SAH  $^{13}\text{C}$  is hyperpolarized by nascent protons three and four chemical bonds away using  $^3J_{\text{H-}^{13}\text{C}}$  and  $^4J_{\text{H-}^{13}\text{C}}$ <sup>[12–13]</sup> versus  $^2J_{\text{H-}^{13}\text{C}}$  and  $^3J_{\text{H-}^{13}\text{C}}$  in conventional PHIP approach<sup>[9, 14]</sup>. As a result, PHIP-SAH significantly expands the reach of amenable to hyperpolarization biomolecules including ethyl acetate-1- $^{13}\text{C}$ , ethyl pyruvate-1- $^{13}\text{C}$  and potentially many others. Ethylation is not necessarily a drawback, because the produced HP contrast agent can be de-protected,<sup>[12]</sup> or used directly, because ethylation of carboxylic acids leads to better cellular<sup>[10b]</sup> and brain uptake.<sup>[15]</sup> The latter is especially relevant to ethyl acetate, because acetate is one of a few metabolites utilized by the brain as a fuel source directly.<sup>[16]</sup>

Despite the potential of PHIP-SAH to revolutionize molecular imaging, it is faced with two fundamental challenges. First, efficient synthesis of vinylated 1- $^{13}\text{C}$ -carboxylates must be developed. Second, % $P_{13\text{C}}$  of only 2.3% (using on 92% of *para*- $\text{H}_2$ ) was achieved by Cavallari et al.,<sup>[13]</sup> and further significant % $P_{13\text{C}}$  boost is required for *in vivo* applications.

Hence, this work is focused on (i) developing an efficient synthetic procedure for production of vinyl acetate-1-<sup>13</sup>C, and (ii) investigating the field cycling polarization transfer process used in PHIP-SAH to improve %  $P_{13C}$ .

A number of methodologies for the preparation of vinyl acetate with various isotopic labeling patterns were previously described. Roberts et al.<sup>[17]</sup> developed a procedure based on mercury-catalyzed reaction of <sup>14</sup>C-labeled acetylene and acetic acid. Similar methodology, based on stoichiometric amount mercury ethoxide and acetyl chloride-*d*<sub>3</sub>, was applied to the preparation of vinyl acetate-*d*<sub>3</sub> by Kim et al.<sup>[18]</sup> Alternatively, Livshits et al.<sup>[19]</sup> showed an efficient reaction between the <sup>14</sup>C labeled acetic acid and acetylene catalyzed by zinc acetate in gas-phase mode. While vinyl acetate is industrially produced by vapor-phase acetoxylation of ethylene over Pd-based catalysts,<sup>[20]</sup> such large-scale gas-phase processes are poorly suited for significantly smaller-scale production of isotopically enriched vinyl acetate-1-<sup>13</sup>C. Earlier variants of synthetic procedures with interexchange of vinyl groups were based on mercury catalysis,<sup>[21]</sup> which had some obvious disadvantages of toxicity and laborious workup. Another potential alternative is based on the recent advances in ruthenium-based catalysis<sup>[22]</sup>. However, equilibrium between vinyl acetate-1-<sup>13</sup>C and its unlabeled counterpart was not directly amenable to the preparation of vinyl acetate-1-<sup>13</sup>C.

Replacement of natural abundance vinyl acetate (**VA**) by vinyl laurate and the application of distillation column allowed for convenient removal of vinyl acetate-1-<sup>13</sup>C (**VA-1-<sup>13</sup>C**) from the reaction mixture (Scheme 1a). Due to the flexible nature of the substrates participating in the vinyl exchange, one can apply this methodology of <sup>13</sup>C enrichment to a variety of potential PHIP targets such as pyruvate and lactate derivatives (Scheme 1b).

We utilized Rh-catalyst ((Bicyclo[2.2.1] hepta-2,5-diene)[1,4-bis(diphenylphosphino)-butane]rhodium(I) tetrafluoroborate) for molecular addition of *para*-H<sub>2</sub> to VA, analogous to one used in the recent PHIP-SAH studies (Figure 1a).<sup>[12-13]</sup> Previously developed setup for high-pressure experiments with *para*-H<sub>2</sub> was utilized (SI),<sup>[23]</sup> demonstrating that higher *para*-H<sub>2</sub> pressure significantly accelerates VA hydrogenation to EA (Figure 1b). Therefore, the highest pressure achievable in this setup (~7.2 bar) was used in further PHIP-SAH experiments. Pairwise addition of 50% *para*-H<sub>2</sub> was performed in the Earth magnetic field (~50 μT) and then the sample was quickly (~2 s) adiabatically transferred to 9.4 T for HP <sup>1</sup>H NMR detection of nascent protons (corresponding to ALTADENA<sup>[24]</sup> conditions). The detected HP <sup>1</sup>H NMR signal initially rises (during fast product build-up) and then decreases (when the contribution of HP product relaxation overweighs formation of new HP species) with the duration of *para*-H<sub>2</sub> bubbling (Figure 1c). The conditions corresponding to bubbling duration of ~8–10 s yielded maximum observed %  $P_H$  of 3.3% (equivalent to <sup>1</sup>H signal enhancement  $_{1H} > 1,000$  fold) and thus, were used to transfer polarization from HP nascent protons to 1-<sup>13</sup>C using magnetic field cycling<sup>[9, 12]</sup> (Figure 1d). In this approach, the pairwise *para*-H<sub>2</sub> addition is performed in the Earth's field, the sample is then quickly moved in a magnetic field <1 μT ( $B_{FC}$ ) and hyperpolarization is transferred to <sup>13</sup>C during slow (adiabatic) sample transfer back to the Earth's field (Figures 1c,d).  $B_{FC}$  adjustment of polarization transfer was carried out by measuring <sup>13</sup>C HP NMR signal of natural abundance EA (~1.1% <sup>13</sup>C in each carbon site) produced by hydrogenation of 80 mM **VA** with *para*-H<sub>2</sub>

(Figure 2e). In-shield field ( $B_{FC}$ ) of 0.1–0.2  $\mu\text{T}$  provided the maximal HP transfer efficiency, and therefore it was used in all subsequent polarization transfer experiments.

The maximum detected  $^{13}\text{C}$  in HP EA was  $> 2,200$  fold for 1- $^{13}\text{C}$  site corresponding to  $\%P_{^{13}\text{C}}$  of  $\sim 1.8\%$  using 50% *para*- $\text{H}_2$  (Figure 1g). A similar  $\%P_{^{13}\text{C}}$  was also achieved for HP  $^{13}\text{C}$  EA-1- $^{13}\text{C}$  (Figure 1h). When compared to natural abundance HP EA, HP  $^{13}\text{C}$  EA-1- $^{13}\text{C}$  carries  $\sim 90\times$  greater polarization payload due to 98%  $^{13}\text{C}$  isotopic enrichment of the  $^{13}\text{C}$  site. The latter was employed for  $^{13}\text{C}$  3D ultra-fast MRI (Figure 2) showing the feasibility of high-resolution (pixel size of  $0.5 \times 0.5 \times 4 \text{ mm}^3$  and  $\sim 2.5 \text{ s}$  duration) molecular imaging with this contrast agent using 15.2 T Bruker MRI scanner.

If  $\sim 100\%$  *para*- $\text{H}_2$ <sup>[25]</sup> would be employed, the effective  $\%P_{\text{H}}$  and  $\%P_{^{13}\text{C}}$  would be tripled to yield 10% and 5.5% respectively. The latter would more than double previously reported pioneering results.<sup>[13]</sup> Moreover, the efficiency of polarization transfer from nascent *para*- $\text{H}_2$  protons to 1- $^{13}\text{C}$  was  $\sim 50\%$ , which is in quantitative agreement with previous theoretical simulation for similar spin system of 2-hydroxyethyl propionate-1- $^{13}\text{C}$ .<sup>[14]</sup> The expected  $\%P_{^{13}\text{C}}$  of  $\sim 5.5\%$  is clearly largely limited by the HP source of  $\%P_{\text{H}}$  of  $\sim 10\%$  in this study and most likely in recent work by Reineri and co-workers.<sup>[13]</sup> Therefore, future studies must focus on the  $\%P_{\text{H}}$  increase and understanding factors leading to the polarization losses. There are three possible major  $\%P_{\text{H}}$ -reducing barriers: (i) the degree of pair-wise addition of *para*- $\text{H}_2$  to vinyl moiety,<sup>[5a, 26]</sup> (ii) nascent protons'  $P$  relaxation, and (iii) singlet-triplet mixing of nascent protons.<sup>[14]</sup> The first challenge is not a fundamental barrier, because similar catalysts yielded  $\%P_{^{13}\text{C}} \sim 30\text{--}50\%$  on similar molecules<sup>[14, 27]</sup> indicating that  $\%P_{\text{H}}$  was 50–100%. On the other hand, the other two barriers have always been previously addressed via the use of high-pressure automated spray-injection PHIP polarizers<sup>[8, 28]</sup> operating at elevated temperatures, and enabling ultra-fast substrate conversion (1–3 s and thereby minimizing the effects of spin-lattice relaxation) and  $^1\text{H}$  decoupling that allows all molecules to retain the singlet states during the course of hydrogenation reaction.<sup>[14]</sup> While additional future studies investigating the reasons behind low  $\%P_{\text{H}}$  in this and previous PHIP-SAH works are certainly warranted, the use of such PHIP polarizers<sup>[8, 28]</sup> will likely provide the remedy and can potentially yield  $\%P_{^{13}\text{C}}$  of up to 50% based on the demonstrated here efficiency of  $\text{H} \rightarrow ^{13}\text{C}$  polarization transfer. Generality and flexibility of trans vinylation approach described here will benefit future efficient preparation of other vinyolated analogs of metabolically relevant compounds such as lactate and pyruvate for PHIP-SAH.<sup>[2a, 2b]</sup> This would pave the way for the future *in vivo* imaging of metabolically impaired conditions such as cancer<sup>[2a, 2b]</sup> and brain<sup>[16]</sup> imaging. In particular, future *in vivo* studies in animal models can be carried out with<sup>[8a]</sup> or without Rh-based PHIP catalysts removal (which are generally well tolerated by animals and cause no clinical toxicity<sup>[29]</sup>) in a manner similar to the previous use of HP succinate-1- $^{13}\text{C}$ <sup>[2e, 8b, 10b]</sup> and HP 2-hydroxyethyl propionate.<sup>[9, 27]</sup> The ultimate clinical translation will require employing Rh-based PHIP catalyst filtration/removal<sup>[8a]</sup> and improving of the filtration/removal step or the alternative use of improved heterogeneous PHIP catalysis.<sup>[26]</sup> Moreover, future *in vivo* translation of this work would require the use of water-soluble catalysts, which have been successfully employed in combination with high-pressure PHIP polarizers<sup>[8, 28]</sup> to produce aqueous solution of HP succinate- $^{13}\text{C}$ ,<sup>[10a]</sup> phospholactate-1- $^{13}\text{C}$ <sup>[3b]</sup> and others with  $\%P_{^{13}\text{C}}$  exceeding 15% and  $T_1$  in excess of 40 s.

## Experimental Section

All experimental procedures, additional NMR spectra as well as the schematic description of the hyperpolarization setup are provided in Supporting Information (SI) for this article.

## Supplementary Material

Refer to Web version on PubMed Central for supplementary material.

## Acknowledgments

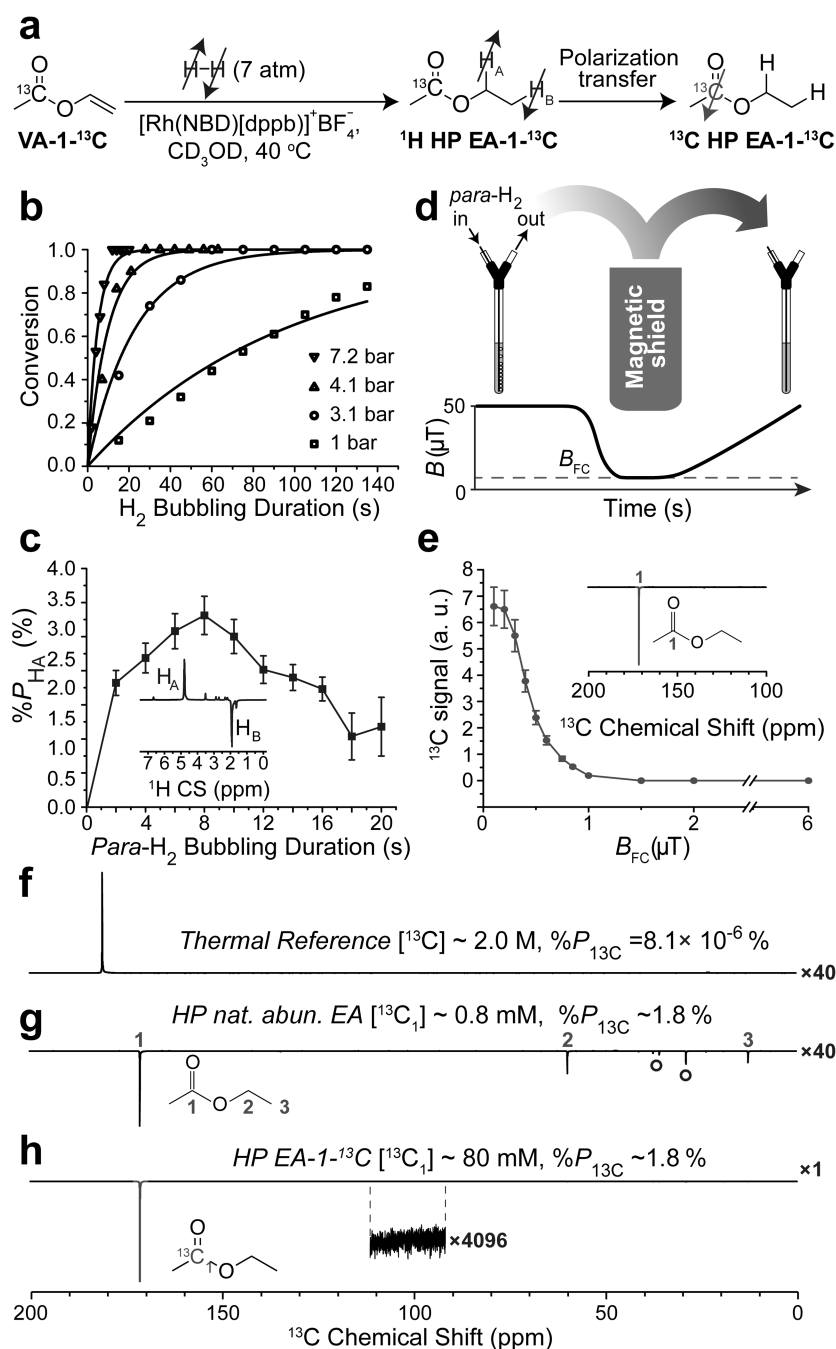
This work was supported by NIH 1R21EB018014 and 1R21EB020323, NSF CHE-1416268, DOD CDMRP W81XWH-12-1-0159/BC112431 and W81XWH-15-1-0271. We are grateful to Oleg Salnikov for preparing the schematic description of hyperpolarization setup in SI.

## References

1. a) Abragam A, Goldman M. *Rep. Prog. Phys.* 1978; 41:395–467. b) Goodson BM. *J. Magn. Reson.* 2002; 155:157–216. [PubMed: 12036331] c) Nikolaou P, Goodson BM, Chekmenev EY. *Chem. Eur. J.* 2015; 21:3156–3166. [PubMed: 25470566]
2. a) Kurhanewicz J, Vigneron DB, Brindle K, Chekmenev EY, Comment A, Cunningham CH, DeBerardinis RJ, Green GG, Leach MO, Rajan SS, Rizi RR, Ross BD, Warren WS, Malloy CR. *Neoplasia.* 2011; 13:81–97. [PubMed: 21403835] b) Brindle KM. *J. Am. Chem. Soc.* 2015; 137:6418–6427. [PubMed: 25950268] c) Comment A, Merritt ME. *Biochemistry.* 2014; 53:7333–7357. [PubMed: 25369537] d) Golman K, in't Zandt R, Thaning M. *Proc. Natl. Acad. Sci. U. S. A.* 2006; 103:11270–11275. [PubMed: 16837573] e) Bhattacharya P, Chekmenev EY, Perman WH, Harris KC, Lin AP, Norton VA, Tan CT, Ross BD, Weitekamp DP. *J. Magn. Reson.* 2007; 186:150–155. [PubMed: 17303454]
3. a) Ardenkjaer-Larsen JH, Fridlund B, Gram A, Hansson G, Hansson L, Lerche MH, Servin R, Thaning M, Golman K. *Proc. Natl. Acad. Sci. U. S. A.* 2003; 100:10158–10163. [PubMed: 12930897] b) Shchepin RV, Coffey AM, Waddell KW, Chekmenev EY. *Anal. Chem.* 2014; 86:5601–5605. [PubMed: 24738968]
4. Nelson SJ, Kurhanewicz J, Vigneron DB, Larson PEZ, Harzstark AL, Ferrone M, van Criekinge M, Chang JW, Bok R, Park I, Reed G, Carvajal L, Small EJ, Munster P, Weinberg VK, Ardenkjaer-Larsen JH, Chen AP, Hurd RE, Odegardstuen LI, Robb FJ, Tropp J, Murray JA. *Sci. Transl. Med.* 2013; 5:198ra108.
5. a) Bowers CR, Weitekamp DP. *Phys. Rev. Lett.* 1986; 57:2645–2648. [PubMed: 10033824] b) Eisenschmid TC, Kirss RU, Deutsch PP, Hommeltoft SI, Eisenberg R, Bargon J, Lawler RG, Balch AL. *J. Am. Chem. Soc.* 1987; 109:8089–8091. c) Bowers CR, Weitekamp DP. *J. Am. Chem. Soc.* 1987; 109:5541–5542.
6. Bornet A, Melzi R, Perez Linde AJ, Hautle P, van den Brandt B, Jannin S, Bodenhausen G. *J. Phys. Chem. Lett.* 2013; 4:111–114. [PubMed: 26291221]
7. Jiang W, Lumata L, Chen W, Zhang S, Kovacs Z, Sherry AD, Khemtong C. *Sci. Rep.* 2015; 5:9104. [PubMed: 25774436]
8. a) Hövener J-B, Chekmenev E, Harris K, Perman W, Robertson L, Ross B, Bhattacharya P. *Magn. Reson. Mater. Phys.* 2009; 22:111–121. b) Hövener J-B, Chekmenev E, Harris K, Perman W, Tran T, Ross B, Bhattacharya P. *Magn. Reson. Mater. Phys.* 2009; 22:123–134.
9. Golman K, Axelsson O, Johannesson H, Mansson S, Olofsson C, Petersson JS. *Magn. Reson. Med.* 2001; 46:1–5. [PubMed: 11443703]
10. a) Chekmenev EY, Hovener J, Norton VA, Harris K, Batchelder LS, Bhattacharya P, Ross BD, Weitekamp DP. *J. Am. Chem. Soc.* 2008; 130:4212–4213. [PubMed: 18335934] b) Zacharias NM, Chan HR, Sailasuta N, Ross BD, Bhattacharya P. *J. Am. Chem. Soc.* 2012; 134:934–943. [PubMed: 22146049]

11. a) Shchepin RV, Coffey AM, Waddell KW, Chekmenev EY. *J. Am. Chem. Soc.* 2012; 134:3957–3960. [PubMed: 22352377] b) Shchepin RV, Pham W, Chekmenev EY. *J. Labelled Comp. Radiopharm.* 2014; 57:517–524. [PubMed: 24995802]
12. Reineri F, Boi T, Aime S. *Nat. Commun.* 2015; 6:5858. [PubMed: 25556844]
13. Cavallari E, Carrera C, Boi T, Aime S, Reineri F. *J. Phys. Chem. B.* 2015; 119:10035–10041. [PubMed: 26161454]
14. Goldman M, Johannesson H. *C. R. Physique.* 2005; 6:575–581.
15. Hurd RE, Yen Y-F, Mayer D, Chen A, Wilson D, Kohler S, Bok R, Vigneron D, Kurhanewicz J, Tropp J, Spielman D, Pfefferbaum A. *Magn. Reson. Med.* 2010; 63:1137–1143. [PubMed: 20432284]
16. Bluml S, Moreno-Torres A, Shic F, Nguy CH, Ross BD. *NMR Biomed.* 2002; 15:1–5. [PubMed: 11840547]
17. Roberts JD, Lee CC, Saunders WH. *J. Am. Chem. Soc.* 1954; 76:4501–4510.
18. Kim JK, Caserio MC. *J. Am. Chem. Soc.* 1982; 104:4624–4629.
19. Livshits VS, Isagulyants GV. *Russ. Chem. Bull.* 1966; 15:1801–1802.
20. a) Kuhn M, Jeschke J, Schulze S, Hietschold M, Lang H, Schwarz T. *Catal. Commun.* 2014; 57:78–82. b) Nakamura S, Yasui T. *J. Catal.* 1970; 17:366–374.
21. Adelman RL. *J. Org. Chem.* 1949; 14:1057–1077.
22. Ziriakus J, Zimmermann TK, Pothig A, Drees M, Haslinger S, Jantke D, Kuhn FE. *Adv. Synth. Catal.* 2013; 355:2845–2859.
23. Truong ML, Theis T, Coffey AM, Shchepin RV, Waddell KW, Shi F, Goodson BM, Warren WS, Chekmenev EY. *J. Phys. Chem. C.* 2015; 119:8786–8797.
24. Pravica MG, Weitekamp DP. *Chem. Phys. Lett.* 1988; 145:255–258.
25. Feng B, Coffey AM, Colon RD, Chekmenev EY, Waddell KW. *J. Magn. Reson.* 2012; 214:258–262. [PubMed: 22188975]
26. Kovtunov KV, Zhivonitko VV, Skovpin IV, Barskiy DA, Koptyug IV. *Top. Curr. Chem.* 2013; 338:123–180. [PubMed: 23097028]
27. Olsson LE, Chai C-M, Axelsson O, Karlsson M, Golman K, Petersson JS. *Magn. Reson. Med.* 2006; 55:731–737. [PubMed: 16538605]
28. a) Waddell KW, Coffey AM, Chekmenev EY. *J. Am. Chem. Soc.* 2011; 133:97–101. [PubMed: 21141960] b) Kadlecsek S, Vahdat V, Nakayama T, Ng D, Emami K, Rizi R. *NMR Biomed.* 2011; 24:933–942. [PubMed: 21845739]
29. Chan, HR.; Bhattacharya, P.; Imam, A.; Freundlich, A.; Tran, TT.; Perman, WH.; Lin, AP.; Harris, K.; Chekmenev, EY.; Ingram, M-L.; Ross, BD. 17th ISMRM Conference; April 18–24; Honolulu, Hawaii: 2009. p. 2448

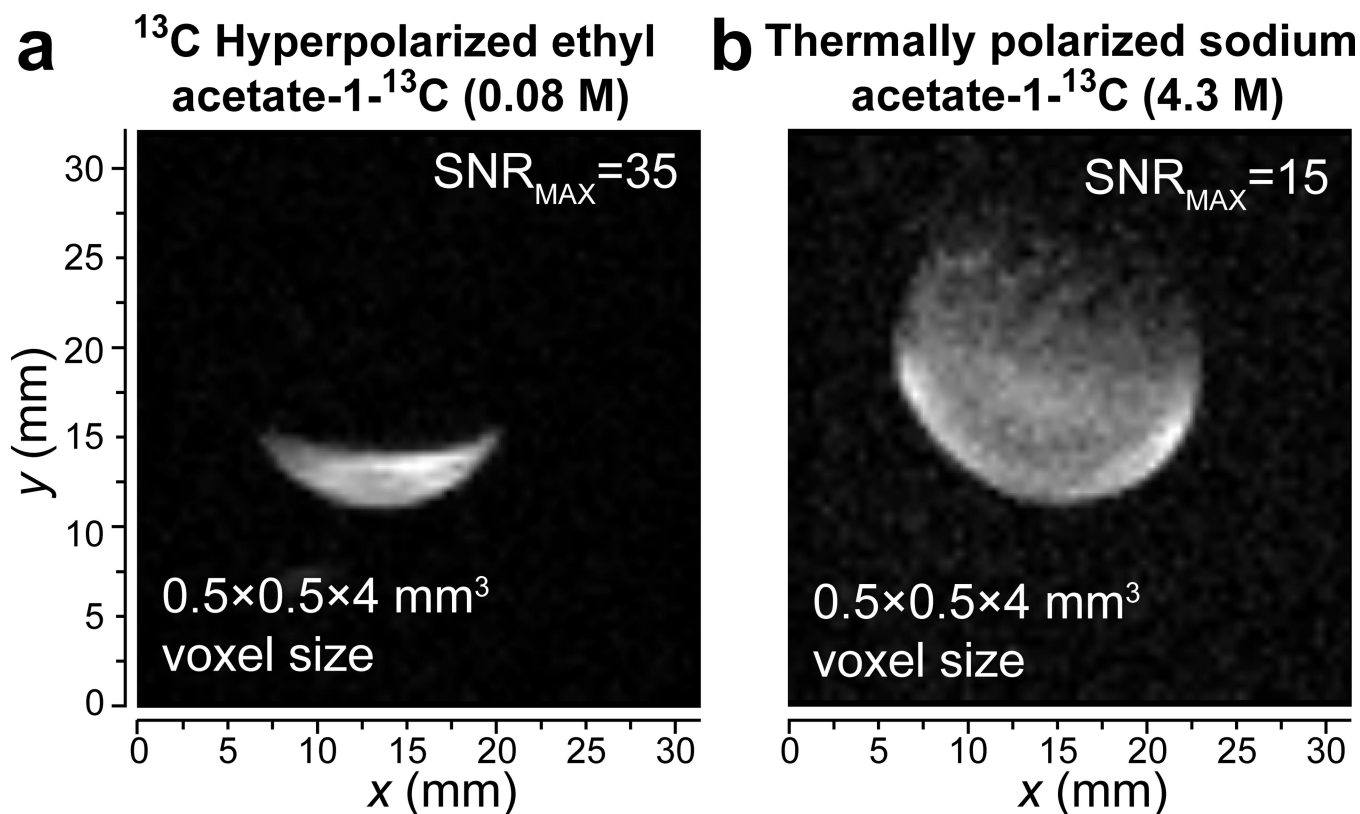




**Figure 1.**  
**a)** Molecular addition of *para*-H<sub>2</sub> to vinyl acetate-1-<sup>13</sup>C (VA-1-<sup>13</sup>C) followed by polarization transfer resulting in <sup>13</sup>C hyperpolarized ethyl acetate-1-<sup>13</sup>C (<sup>13</sup>C HP EA-1-<sup>13</sup>C); **b)** Conversion profile for vinyl acetate (VA, 80 mM, in methanol-*d*<sub>4</sub>, at ~40 °C temperature maintained by the 9.4 T NMR spectrometer) hydrogenation reaction in four pressure regimes; **c)** Dependence of “H<sub>A</sub>” signal of hyperpolarized ethyl acetate (<sup>1</sup>H HP EA) on the *para*-H<sub>2</sub> bubbling duration at the Earth’s magnetic field (resulting in ALTADENA<sup>[24]</sup>-type spectrum shown in inset); **d)** (Top) schematic representation of experimental setup for

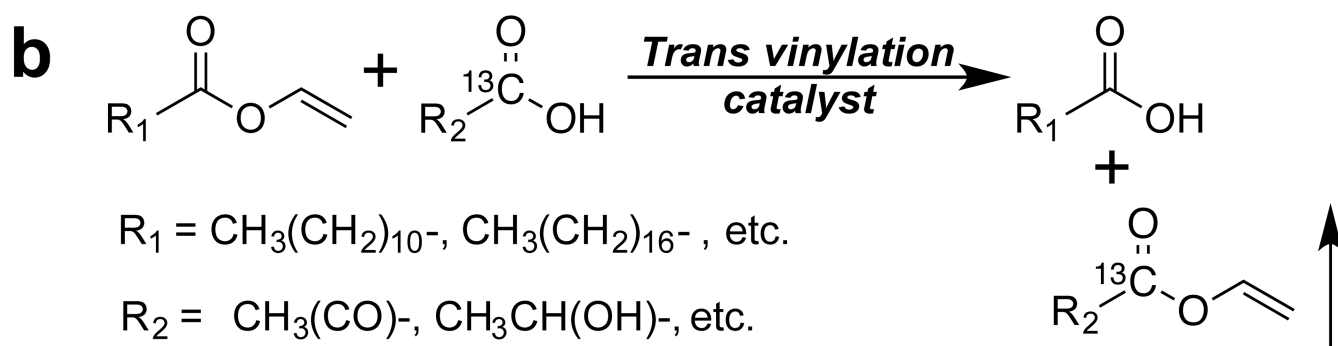
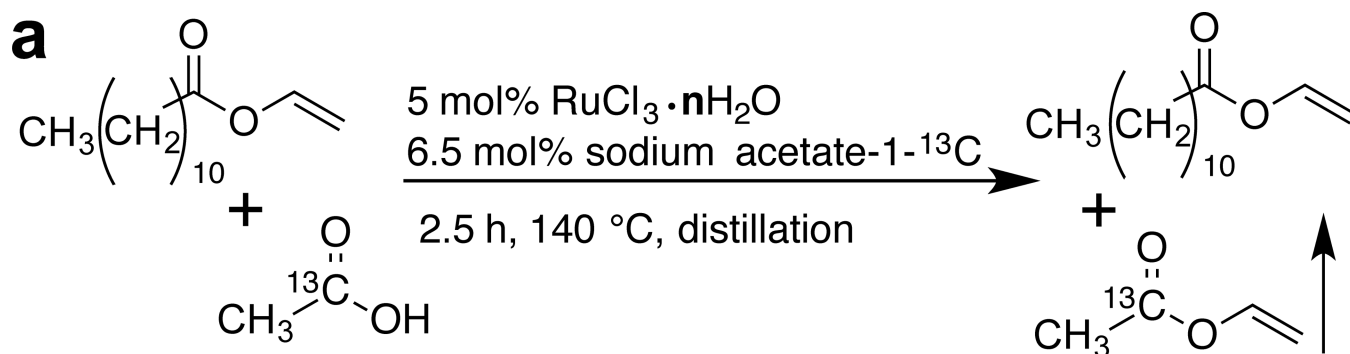
magnetic field cycling: hydrogenation is carried out at the Earth's magnetic field, the sample then is quickly moved inside -metal shield (with magnetic field  $B_{FC}$ ) and slowly transferred from the shield for subsequent NMR detection; (bottom) schematic magnetic field profile during the field cycling; **e**) Dependence of HP  $1-^{13}\text{C}$  NMR signal (shown in the insert) of ethyl acetate ( $^{13}\text{C}$  **HP EA**) on the  $B_{FC}$ ; **f**) Thermal spectrum of  $^{13}\text{C}$  signal reference sodium acetate- $1-^{13}\text{C}$  (~2.0 M); **g**)  $^{13}\text{C}$  HP spectrum of natural abundance 80 mM ethyl acetate ( $^{13}\text{C}$  **HP EA**). Note the resonances labeled with  $^\circ$  correspond to HP  $^{13}\text{C}$  resonances originating from hydrogenation catalyst (Figure S7); **h**) HP  $^{13}\text{C}$  spectrum of 80 mM ethyl acetate- $1-^{13}\text{C}$  ( $^{13}\text{C}$  **HP EA-1- $^{13}\text{C}$** ).





**Figure 2.**

$^{13}\text{C}$  3D MRI of (a) a hollow spherical plastic ball partially filled with 80 mM HP EA- $1\text{-}^{13}\text{C}$  and (b) a plastic sphere (~2.8 mL) filled with thermally polarized 4.3 M sodium acetate- $1\text{-}^{13}\text{C}$  reference phantom. Both 3D true-FISP images were acquired using 15 mm OD round RF surface coil tuned to 163.4 MHz in 15.2 T small-animal Bruker MRI scanner (see SI for additional details). One representative slice is shown for each 3D image.

**Scheme 1.**

**a)** Reaction scheme for the preparation of vinyl acetate-1- $^{13}\text{C}$  (VA-1- $^{13}\text{C}$ ). **b)** Generalized scheme for preparation of potential targets with vinylated carboxyl groups.